3686 *J. Phys. Chem. A* **2007,** *111,* 3686−3690

ARTICLES

OH-Initiated Oxidation of Toluene. 1. Quantum Chemistry Investigation of the Reaction Path[†]

Terry J. Frankcombe*

Leiden Institute of Chemistry, Gorlaeus Laboratories, Leiden University, P.O. Box 9502, 2300 RA Leiden, The Netherlands

Sean C. Smith[‡]

Centre for Computational Molecular Science, University of Queensland, St. Lucia, Queensland 4072, Australia

Received: October 30, 2006; In Final Form: December 6, 2006

In this paper we present the results of a detailed quantum chemistry investigation of the toluene−OH−O_2 system, mostly at the B3LYP/6-311G(2df,2pd) level. We focus on OH addition followed by H abstraction to O_2, a mechanism based on that proposed by Klotz et al. [*Phys. Chem. Chem. Phys.* **2000**, *2*, 227] to explain the experimentally observed photolysis products. A notable feature of the calculated minimum energy pathway is the formation of ketone intermediates during the isomerization from the toluene oxides to the cresols. The quantum chemistry results largely support the plausibility of the mechanism proposed by Klotz et al. The system provides a rich set of reactions with which to test statistical kinetic theories.

1. Introduction

Toluene is the most abundant aromatic species in the atmosphere.[1−4] The photo-oxidation of airborne aromatic species, and toluene in particular, is a major source of atmospheric ozone in urban environments.[2,4−8] Additionally, the degradation of toluene and other aromatic species can lead to the formation of secondary organic aerosols.[1,2,8,9] Thus the understanding of the atmospheric chemistry of toluene is of great importance. Despite this, degradation mechanisms of atmospheric toluene are not well-known. On the basis of photo-oxidation data, Klotz et al. proposed a mechanism for the oxidation and degradation of toluene that proceeds by successive reactions with OH radicals and removal of hydrogen by O_2.[10] The bulk of the proposed mechanism remains speculative and based on the interpretation of kinetic data.

The toluene + OH reaction itself has been studied previously using computational methods. Bartolotti and Edney,[11] García-Cruz and co-workers[3,12] and Suh et al.[2,13] have performed quite similar investigations, looking at the initial attack of OH on toluene and subsequent addition reactions with O_2, using wavefunction- and density functional-based methods. Qualitatively in accord with experimental evidence,[14] the probability of forming non-ortho products is found to be small, but significant. Wavefunction-based methods are found to be problematic for this system. These studies have also shown that including zero-point energy contributions to the energetics for the stationary points involved with the initial toluene + OH reaction significantly alters the calculated branching ratios for the isomeric products with the OH fragment attached at different places on the toluene ring.

Predating most of the studies mentioned above, Andino et al.[15] performed extensive exploration of the OH-mediated degradation of toluene, studying not only the subsequent O_2 addition but also some potential pathways following reaction with NO_x. Using density functional and semiempirical methods, the authors again focused on the addition of O_2 to the toluene hydroxide product, which predominantly forms bicyclic peroxyl radicals. No quantum chemistry investigations have been performed that elucidate reactive pathways to the toluene breakdown products observed experimentally by Klotz et al.[10]

In this work we explore the potential energy surface on which OH-initiated photo-oxidation occurs. We start from toluene + OH and base our exploration of the reaction mechanism on that proposed by Klotz et al.[10] Characterization of the stationary points along the minimum energy pathways of the reaction mechanism is an essential step in the modeling of the reaction using statistical methods,[16−18] which shall be published in the accompanying paper.[19] In particular, with its large network of coupled unimolecular and simple bimolecular reactions the toluene−OH−O_2 system provides a lot of scope for testing master equation modeling methods for multiple species systems.

2. Methods

The Gaussian 03 package[20] was used for all calculations. Calculations were performed at the B3LYP/6-311G(2df,2pd) level of theory. A number of recent studies have concluded that the B3LYP hybrid density function gives more accurate energies than more computationally expensive ab initio methods (such as Møller−Plesset and coupled cluster methods) for the toluene + OH reaction and related oxygen-containing systems.[2,12,13] The

---

[†] Part of the special issue “James A. Miller Festschrift”.

* Corresponding author. E-mail: T.Frankcombe@chem.leidenuniv.nl.

[‡] E-mail: S.Smith@uq.edu.au.

10.1021/jp067112i CCC: $37.00

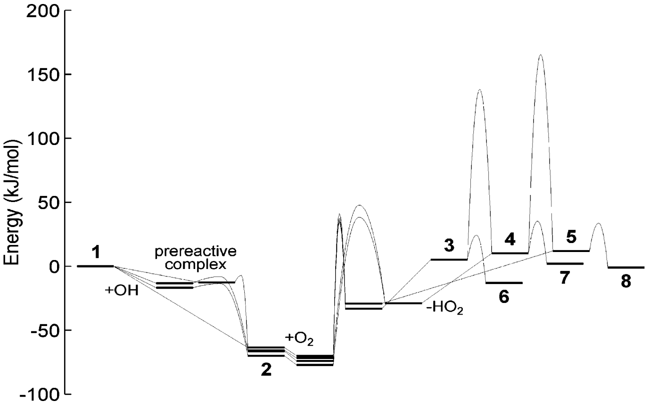

Figure 1. Calculated MEP of the OH-mediated first oxidation step of toluene.

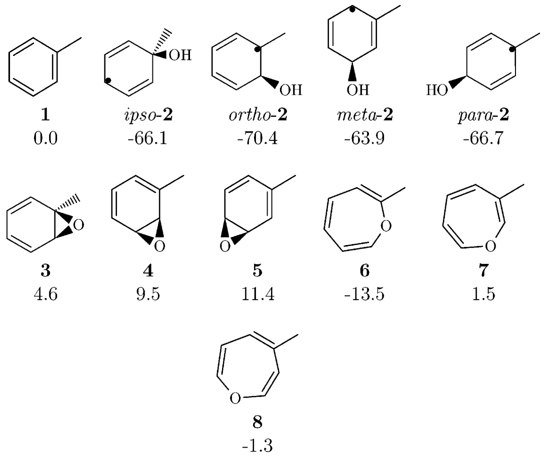

Figure 2. Species involved in the OH-mediated first oxidation step of toluene and the relative ZPE-corrected ground state energy (kJ/mol).

relatively large basis set has been used to reduce basis set truncation and basis set superposition errors.

For all species and configurations considered the geometry was relaxed to give the minimum energy configuration. Except in the well-known case of O_2, the lowest multiplicity spin state (singlet or doublet) was consistently found to be the lowest in energy. For all the reaction paths considered, saddle points on the minimum energy paths (MEPs) were deemed to be transition states and located using the STQN method.[21,22] Most transition states were confirmed with the IRC reaction path following algorithm.[23] Unless otherwise noted, all energies reported here have zero-point energy (ZPE) included with the ZPE contribution being calculated by harmonic vibrational analysis. All energies are plotted relative to the energy of the initial toluene system (with appropriate free O_2 and OH radical energies added).

3. Minimum Energy Reaction Path

3.1. First Oxidation Step. According to the proposed mechanism of Klotz et al.,[10] the first step is the addition of an OH radical to the toluene (**1**) ring followed by donation of the hydrogen atom of the added OH fragment to an O_2 molecule. Clearly there are four positions to which the OH radical can bond to form the hydroxycyclohexadienyl radical **2**, corresponding to the four non-equivalent unsaturated carbons in the toluene ring. The calculated MEP of these reactions are represented in Figure 1, and Figure 2 shows the species involved (excluding the van der Waals complexes with O_2 and HO_2).

Like in previously published results, OH addition in the ortho position was found to be more stable than addition to other positions. Addition in the ipso, meta and para positions were found to be 4.3, 6.5 and 3.6 kJ/mol less stable, respectively, than the −70.4 kJ/mol binding energy associated with the ortho position. This is again consistent with previous B3LYP results but qualitatively different from MP2 and coupled cluster results, which show the ipso structure to be more stable, though the accuracy of MP2 for this system has been questioned.[2,3,12,13] The B3LYP binding energy for the addition of the OH fragment calculated here was about 3.5 kJ/mol smaller than that calculated previously using a smaller basis set.[2]

The OH addition reaction in general proceeds through loosely bound toluene−OH collision complexes. The binding energies of these complexes were of the order of 15 kJ/mol, but the barriers to proceed from the complexed states to the hydroxylated products were found to be small, just 3−5 kJ/mol. Possibly because of the shallowness of these wells no pre-reactive complex leading to OH addition in the meta position was found.

Although previous studies[3,13,15] have followed Atkinson et al.[24] and focused on the reactive addition of O_2 to the hydroxylated product, in this work we follow Klotz et al.[10] and consider H abstraction by O_2 to form HO_2. One conceivable mechanism of this abstraction is reactive O_2 addition to **2**, followed by migration of H to the end of the added O_2 fragment and dissociation of HO_2. Species with O_2 added end-on to unsaturated sites of **2** and with the H atom from the OH group migrated to the added group were found to be stable. However, the minimum energy paths as the carbon−oxygen bonds were stretched and broken to release the HO_2 were found to involve donation of the H atom back to the toluene oxide in all cases. Thus we consider not reactive O_2 addition but complex-forming O_2 addition. The isomers of **2** each form a stable van der Waals complex with O_2 with a binding energy of 6−7.5 kJ/mol. Once the complex with O_2 forms the added OH fragment can dissociate to form a complex of HO_2 bound to toluene oxide. Three toluene oxide isomers can form [toluene-1,2-oxide (**3**), toluene-2,3-oxide (**4**) and toluene-3,4-oxide (**5**)], with the oxygen atom bridging one of the three non-equivalent carbon−carbon bonds of the toluene. Forming the oxide involves the oxygen atom forming a bond with a carbon atom adjacent to the carbon atom to which it is already bound, thus although only one isomer can result from each of the ipso and para adducts, the ortho and meta hydroxylated structures can each form two toluene oxide isomers. The saddle point energies for these toluene oxide-forming reactions were found to be rather high. Getting over these barriers would require significantly more energy than is liberated in the OH addition reaction and O_2 complexation.

Once the HO_2-containing complex has dissociated, several isomerization paths are open to the toluene oxide. As proposed by Klotz et al.,[10] given sufficient energy the oxide can migrate around the ring, interconverting the three oxides. The three oxides can convert to monocyclic methyloxepins (**6**, **7** and **8**) effectively by opening the three-membered ring where the oxide is bound across a carbon−carbon bond. The barriers for these ring-opening isomerizations are relatively low and the methyloxepins are more stable than the toluene oxides by 8−18 kJ/mol, consistent with a rapidly attained equilibrium between the toluene oxides and methyloxepins that favors the methyloxepins.[10,25,26]

3.2. Ketone and Cresol Formation. In addition to isomerization between the toluene oxides and ring opening to methyloxepins, the toluene oxides **3**, **4** and **5** can isomerize to form cresol (**9**, **10** and **11**). Klotz et al.[10] proposed that the cresol isomers could form directly from the toluene oxides by hydrogen migration. However, they also observed a major product that

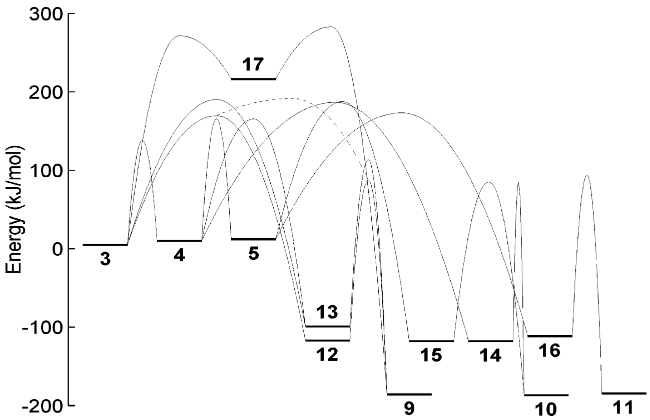

Figure 3. Calculated MEP of ketone and cresol formation from toluene oxide. Dashed line indicates approximate methylcyclohexenone bypass path (see text).

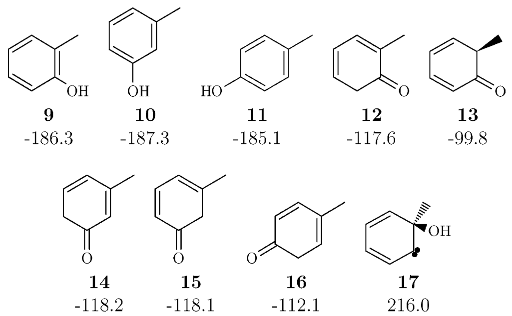

Figure 4. Species involved in ketone and cresol formation from toluene oxide and the relative ZPE-corrected ground state energy (kJ/mol).

could not be identified but exhibited a spectrum characteristic of ketenes/carbonyls.

The MEPs calculated in this work (Figure 3) do not support the direct formation of cresol isomers from toluene oxide. All attempts to find a transition state on such a reaction path lead instead to transition states that lead from toluene oxides to methylcyclohexenone isomers. Along these reaction paths a hydrogen atom bonded to a carbon center participating in the epoxide bond of toluene oxide migrates to an adjacent carbon site. At the same time the formerly epoxide oxygen atom forms a ketone double bond to the vacated carbon atom. This rather complex MEP was confirmed at the MP2 level. The three toluene oxide isomers give rise to five possible ketone isomers, **12**−**16** (Figure 4). These are newly identified candidates for the major products observed by Klotz et al. that were attributed to ketene/carbonyl species. From the five ketone isomers the cresols can form by hydrogen migration from the saturated carbon back onto the oxygen to form the hydroxy group. As can be seen from Figure 3, these hydrogen migration reactions are relatively high-energy processes, but the resultant ketones and cresols are significantly more stable than the proceeding species back along the reaction path.

From toluene-1,2-oxide (**3**) two additional paths leading to *o*-cresol (**9**) were investigated. First, a path between the saddle points on the **3** → **12** and **12** → **9** paths was constructed by a simple linear interpolation of the atomic positions. This path simply bypasses the potential well of **12** and serves as a measure of the energy penalty of moving away from the MEP. It was found that such a bypass would require approximately 22 kJ/mol higher energy than passing along the MEP. This figure does not include any ZPE corrections, adding an additional level of approximation to the linear interpolation. The energetics of such a bypass are indicated by the dashed line connecting the relevant saddle points in Figure 3. The second path from **3** to **9** proceeded via a diradical structure **17** in which the hydroxy group of the cresol had already formed, albeit on a different carbon center. Not surprisingly, this path required significantly higher energy than the non-radical paths. Similar paths were not investigated for the other isomers.

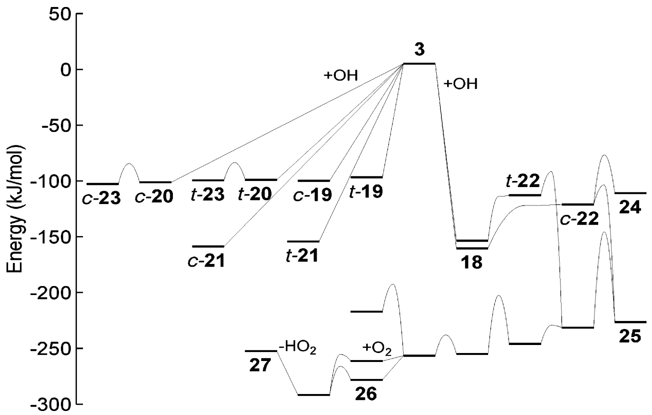

Figure 5. Calculated MEP of the OH-initiated oxidation of toluene-1,2-oxide (**3**).

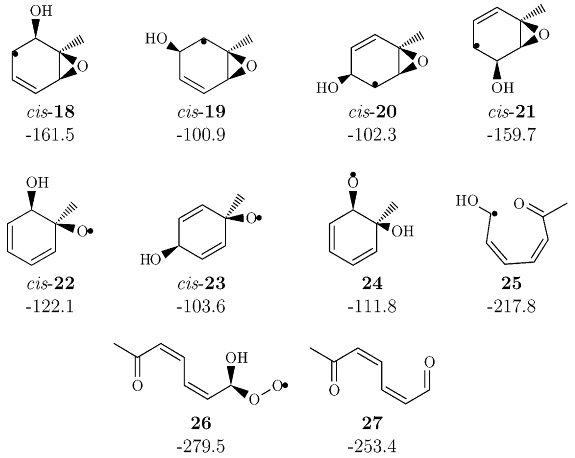

Figure 6. Species involved in the OH-initiated oxidation of toluene-1,2-oxide (**3**) and the relative ZPE-corrected ground state energy (kJ/mol). (Only cis isomers shown.)

3.3. Second Oxidation Step. Klotz et al.[10] observed the formation of 6-oxohepta-2,4-dienal when toluene-1,2-oxide (**3**) was further oxidized with OH again serving as an initiator. We have explored the proposed mechanism with some extensions. Both toluene-1,2-oxide (**3**) itself and the 2-methyloxepin (**6**) with which it is in equilibrium need to be considered. We do not consider the other toluene oxide or methyloxepin isomers here, as a mechanism of OH/O_2 attack on those isomers leading to 6-oxohepta-2,4-dienal would be considerably more complicated. The MEP for the oxidation starting from toluene-1,2-oxide is represented in Figure 5 and the involved species are shown in Figure 6.

There are four sites to which the attacking OH group can attack in toluene-1,2-oxide (**3**), each of which having the possibility of the OH group cis or trans to the epoxide. There is no pre-reactive complex of **3** with the incoming OH group for this reaction, giving a simple barrierless association reaction liberating around 160 kJ/mol for addition to carbon atoms adjacent to the epoxide (**18** and **21**) and around 105 kJ/mol for addition to the more distant sites (**19** and **20**). The next step in the mechanism sees migration of the radical site to the epoxide oxygen atom to break one of the carbon−oxygen bonds. This

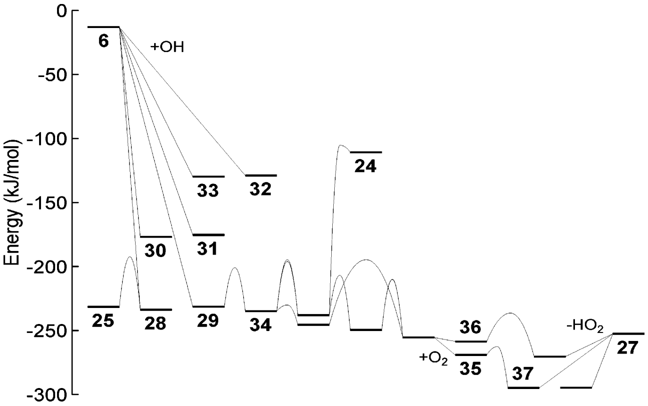

Figure 7. Calculated MEP of the OH-initiated oxidation of 2-methyloxepin (**6**).

isomerization was only found to be possible for isomers **18** and **20** in which the originating radical site is meta to the methyl group adjacent to the epoxide, leading to **22** and **23**. No stable species could be found that would arise from the radical migration from **19** or **21**. Location of the transition states for the **18** → **22** isomerizations presented an additional complication. Although the saddle points on the reaction paths were located easily, applying ZPE corrections to those points resulted in energies lower than those of the products **22** once ZPE corrections had been applied. Scanning along the MEPs using the IRC algorithm and calculating the ZPE-corrected energy along those paths (using vibrational frequencies for normal modes with the mass-weighted direction of the reaction path projected out) confirmed that there were indeed ZPE-corrected energy maxima along the IRC paths, just slightly above the energies of the isomers of **22**.

The products of OH attack at the position para to the methyl group (via **20** and **23**) were not investigated further as only the significantly more stable **22** can lead to 6-oxohepta-2,4-dienal via a reasonable reaction path. From the cis form of **22** the hydroxy hydrogen atom can migrate to the radical oxygen site to form **24**, a species that can ring open to join the reaction path from OH addition to 2-methyloxepin (**6**), which shall be discussed below. Ring opening of **22** leads to an oxoheptenol **25**, of which six conformers (and the saddle points through which the interconvert) have been identified. The most stable conformer of **25** lies almost 100 kJ/mol lower in energy than **18**, the OH-addition product leading to it from toluene oxide.

Unlike the hydrogen extraction that occurs as part of the first oxidation step, the abstraction of the hydroxy H atom by O_2 can occur via an O_2 loosely bound in a van der Waals complex or via O_2 bound in a peroxyl radical (**26**). However transferring the hydrogen atom from the hydroxy group to the radical site can only be achieved by simultaneous dissociation of the nascent HO_2 into a van der Waals complex, the same complex that arises when the transfer is to a complexed (rather then bound) O_2 molecule. Dissociation of the HO_2 complex (in which the HO_2 fragment is hydrogen-bound to the terminal, aldehyde oxygen) leads to an isomer of 6-oxohepta-2,4-dienal (**27**), the observed product.

From the 2-methyloxepin (**6**) isomer that is on the favored side of the equilibrium with toluene oxide (**3**), the OH radical can attack any of the six carbon sites. Klotz et al. considered only addition to carbons 2 and 7, adjacent to the oxygen. The resulting structures (**28** and **29**) turn out to be the most stable with the association liberating around 220 kJ/mol (Figures 7 and 8). Like the addition to toluene oxide, the lack of aromaticity in the ring means that there is no pre-reactive van der Waals complex. Addition at the 4 and 5 positions (**30** and **31**) gives structures around 56 kJ/mol higher in energy. Addition at the 3 and 6 positions (**32** and **33**) gives more puckered ringed structures a further 45 and 48 kJ/mol less stable. These less thermodynamically favoured structures do not lead to the formation of the observed product and were not considered further.

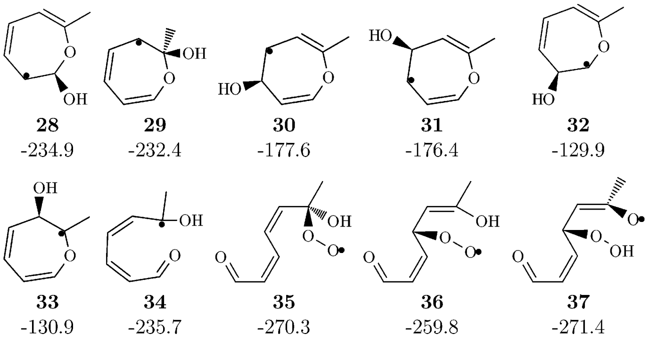

Figure 8. Species involved in the OH-initiated oxidation of 2-methyloxepin (**6**) and the relative ZPE-corrected ground state energy (kJ/mol).

From the product of OH addition to carbon 2 (**28**), ring cleavage leads to oxoheptenol (**25**). As discussed above, H abstraction via O_2 leads to the 6-oxohepta-2,4-dienal product.

Ring opening of the other stable **6**+OH product (**29**) leads to **34**, of which five conformers have been characterized. Two interconversions within these conformers can occur via two different pathways of similar energy, corresponding to internal rotation in two different directions. One conformer of **34** is the product of the ring opening of **24**, lying on the reaction path from addition of OH to toluene oxide, discussed above. There were indications that, like **25**, the H abstraction from **34** by O_2 could potentially occur either via a van der Waals complex or through a peroxyl radical after addition of O_2 to **34**. It seems that the migration to complexed O_2 gives the lowest reaction pathway. However, we were unable to precisely locate the saddle point along the complex-to-complex reaction path. Hydrogen transfer to the radical site can occur after O_2 addition to either the second or the fourth carbon in the chain, to form **35** or **36**, respectively. From **36** the hydroperoxide **37** can form, followed by HO_2 removal to form the product **27**. On the other hand the hydrogen migration from **35** is associated with breaking of the carbon-oxygen bond, like that observed for the analogous process from **26**. The resulting complex of **27** with HO_2 is a different configuration to that resulting from the lowest energy pathway removing the hydrogen atom to a complexed O_2. The potential products of O_2 addition at the other carbons that could lead to the hydroperoxide without large amplitude motion, the third and fifth, were found not to be stable.

4. Conclusion

In this work a total of 121 stationary points have been determined on the B3LYP/6-311G(2df,2pd) potential energy surface of the $C_7H_8 + 2OH + 2O_2$ system (70 minima and 51 saddle points). The detailed geometries, energies and vibrational frequencies are given in the accompanying Supporting Information.

Where previous calculations have been done (namely for the initial toluene + OH reaction mostly via a pre-reactive complex) the current energetics and structures were found to be similar. Rather than following the addition of O_2 to the toluene hydroxide products and subsequent isomerization, we have followed the mechanism proposed by Klotz et al.[10] aiming toward the formation of the products observed experimentally by removing hydrogen to form toluene oxides.

The energetics determined in this work were broadly consistent with the mechanism proposed by Klotz et al. There were, however, some notable differences. First, there is no compelling evidence that OH addition to toluene at positions other than the ortho position should be excluded from future kinetic modeling of the system. Although the ortho adduct leading to toluene-1,2-oxide will certainly dominate, the toluene oxide branching fractions to toluene-2,3-oxide and toluene-3,4-oxide are likely to be non-negligible.

Second, both the hybrid DFT functional and MP2 potential energy surfaces indicate that there are deep wells along the MEPs from the toluene oxides to the cresols. These wells correspond to ketone structures. These MEPs were found to be rather unusual pathways, with hydrogen migration from one carbon atom to an adjacent one to allow the ketone to form, before reverse migration to form the hydroxide on the former ketone site. Although moving off the MEP and circumventing these wells to give direct formation of the cresols as proposed by Klotz et al. did not appear to cost much energy (relative to the reasonably high barriers along the MEP) so that when not constrained to the MEP one should expect some direct cresol formation, the ketone intermediates will almost certainly be formed. Determining whether these intermediates will be formed in more than minor amounts is not obvious from the energetics and will require investigation of the kinetics of the reactions.

Finally, in this work a lot of detail has been filled in about the stationary points along the reaction path from toluene oxide/methyloxepin to the observed product, 6-oxohepta-2,4-dienal, via OH addition and H abstraction by O_2. Many isomers of the ring opened $C_7H_9O_2$ species, in particular, have been characterized.

It is worth emphasising that the reaction path investigated in this work closely followed that proposed by Klotz et al. No alternative pathways were considered, other than logical extensions (in the case of addition at non-ortho sites) and adding necessary minima (the ketones discovered on the toluene oxide to cresol paths). In the context of atmospheric chemistry, high reaction barriers were found along the pathway. The hydrogen abstractions to O_2 leading to the formation of the toluene oxides presented barriers around 40 kJ/mol above the energy of the toluene entrance channel. Worse, formation of the ketones **12**−**16** from the toluene oxides exhibited barriers all greater than 150 kJ/mol above the toluene oxide energies. Any pathways from toluene + OH leading to 6-oxohepta-2,4-dienal **27** or the cresols **9**−**11** that avoid the formation of toluene oxide are likely to compete effectively with the paths proposed by Klotz et al. and presented here.

Though interesting in its own right, the OH-initiated oxidation of toluene yields a fertile ground for selecting multiple species systems for testing kinetics modeling methods.[27] This shall be explored further in the following accompanying paper,[19] along with the general kinetic behavior of the isomerization of the toluene oxides/methyloxepins.

Supporting Information Available: Geometries, energies and frequencies of the stationary points described in this work have been compiled into a PDF document. This material is available free of charge via the Internet at http://pubs.acs.org.

References and Notes

(1) Hurley, M. D.; Sokolov, O.; Wallington, T. J.; Takekawa, H.; Karasawa, M.; Klotz, B.; Barnes, I.; Becker, K. H. *Environ. Sci. Technol.* **2001**, *35*, 1358.

(2) Suh, I.; Zhang, D.; Zhang, R.; Molina, L. T.; Molina, M. J. *Chem. Phys. Lett.* **2002**, *364*, 454.

(3) García-Cruz, I.; Castro, M.; Vivier-Bunge, A. *J. Comput. Chem.* **2000**, *21*, 716.

(4) Huang, M.; Zhang, W.; Yang, Y.; Wang, Z.; Hao, L.; Zhao, W.; Zhao, W.; Li, J.; Gao, X. *J. Mol. Struct. (THEOCHEM)* **2006**, *774*, 1.

(5) Derwent, R. G.; Jenkin, M. E.; Saunders, S. M. *Atmos. Environ.* **1996**, *30*, 181.

(6) Xiao, H.; Zhu, B. *Water Air Soil Pollut.* **2003**, *145*, 3.

(7) Bloss, C.; Wagner, V.; Bonzanini, A.; Jenkin, M. E.; Wirtz, K.; Martin-Reviejo, M.; Pilling, M. J. *Atmos. Chem. Phys.* **2005**, *5*, 623.

(8) Volkamer, R.; Jimenez, J. L.; San Martini, F.; Dzepina, K.; Zhang, Q.; Salcedo, D.; Molina, L. T.; Worsnop, D. R.; Molina, M. J. *Geophys. Res. Lett.* **2006**, *33*, L17811.

(9) Atkinson, R. *Atmos. Environ.* **2000**, *34*, 2063.

(10) Klotz, B.; Barnes, I.; Golding, B. T.; Becker, K.-H. *Phys. Chem. Chem. Phys.* **2000**, *2*, 227.

(11) Bartolotti, L. J.; Edney, E. O. *Chem. Phys. Lett.* **1995**, *245*, 119.

(12) Uc, V. H.; García-Cruz, I.; Hernández-Laguna, A.; Vivier-Bunge, A. *J. Phys. Chem. A* **2000**, *104*, 7847.

(13) Suh, I.; Zhang, R.; Molina, L. T.; Molina, M. J. *J. Am. Chem. Soc.* **2003**, *125*, 12655.

(14) Kenley, R. A.; Davenport, J. E.; Hendrey, D. G. *J. Phys. Chem.* **1981**, *85*, 2740.

(15) Andino, J. M.; Smith, J. N.; Flagan, R. C.; Goddard, W. A., III; Seinfeld, J. H. *J. Phys. Chem.* **1996**, *100*, 10967.

(16) Gilbert, R. G.; Smith, S. C. *Theory of Unimolecular and Recombination Reactions;* Blackwell Scientific: Oxford, U.K., 1990.

(17) Frankcombe, T. J.; Smith, S. C.; Gates, K. E.; Robertson, S. H. *Phys. Chem. Chem. Phys.* **2000**, *2*, 793.

(18) Frankcombe, T. J.; Smith, S. C. *Faraday Discuss.* **2002**, *119*, 159.

(19) Frankcombe, T. J.; Smith, S. C. *J. Phys. Chem. A* **2006**, *111*, 3691.

(20) Frisch, M. J.; Trucks, G. W.; Schlegel, H. B.; Scuseria, G. E.; Robb, M. A.; Cheeseman, J. R.; Montgomery, J. A., Jr.; Vreven, T.; Kudin, K. N.; Burant, J. C.; Millam, J. M.; Iyengar, S. S.; Tomasi, J.; Barone, V.; Mennucci, B.; Cossi, M.; Scalmani, G.; Rega, N.; Petersson, G. A.; Nakatsuji, H.; Hada, M.; Ehara, M.; Toyota, K.; Fukuda, R.; Hasegawa, J.; Ishida, M.; Nakajima, T.; Honda, Y.; Kitao, O.; Nakai, H.; Klene, M.; Li, X.; Knox, J. E.; Hratchian, H. P.; Cross, J. B.; Adamo, C.; Jaramillo, J.; Gomperts, R.; Stratmann, R. E.; Yazyev, O.; Austin, A. J.; Cammi, R.; Pomelli, C.; Ochterski, J. W.; Ayala, P. Y.; Morokuma, K.; Voth, G. A.; Salvador, P.; Dannenberg, J. J.; Zakrzewski, V. G.; Dapprich, S.; Daniels, A. D.; Strain, M. C.; Farkas, O.; Malick, D. K.; Rabuck, A. D.; Raghavachari, K.; Foresman, J. B.; Ortiz, J. V.; Cui, Q.; Baboul, A. G.; Clifford, S.; Cioslowski, J.; Stefanov, B. B.; Liu, G.; Liashenko, A.; Piskorz, P.; Komaromi, I.; Martin, R. L.; Fox, D. J.; Keith, T.; Al-Laham, M. A.; Peng, C. Y.; Nanayakkara, A.; Challacombe, M.; Gill, P. M. W.; Johnson, B.; Chen, W.; Wong, M. W.; Gonzalez, C.; Pople, J. A. *Gaussian 03*; Gaussian, Inc.: Pittsburgh, PA, 2003.

(21) Peng, C.; Schlegel, H. B. *Isr. J. Chem.* **1994**, *33*, 449.

(22) Peng, C.; Ayala, P. Y.; Schlegel, H. B.; Frisch, M. J. *J. Comput. Chem.* **1996**, *17*, 49.

(23) Gonzalez, C.; Schlegel, H. B. *J. Phys. Chem.* **1990**, *94*, 5523.

(24) Atkinson, R.; Carter, W. P. L.; Darnall, K. R.; Winer, A. M.; Pitts, J. N., Jr. *Int. J. Chem. Kinet.* **1980**, *12*, 779.

(25) Vogel, E.; Günther, H. *Angew. Chem.* **1967**, *79*, 429.

(26) Günther, H.; Schubarth, R.; Vogel, E. *Z. Naturforsch. B* **1967**, *22*, 25.

(27) Frankcombe, T. J.; Smith, S. C. *J. Theor. Comput. Chem.* **2003**, *2*, 179.